RICE HUSK ASH SILICA AS A SUPPORT MATERIAL FOR RUTHENIUM BASED HETEROGENOUS CATALYST

Farook Adam*, Saraswathy Balakrishnan and Phee-Lee Wong

School of Chemical Sciences, Universiti Sains Malaysia,
11800 USM Pulau Pinang, Malaysia

*Corresponding author: farook@usm.my

Abstract: *Heterogeneous ruthenium catalysts supported on silica from rice husk ash (RHA-Ru) was prepared by precipitation using an aqueous solution of metal salt in 3.0 M HNO_3. The effect of calcination at high temperature upon the surface and bulk structure of the catalyst precursor has been investigated. X-ray diffraction studies on RHA-Ru showed that it existed in an amorphous state. However, on calcination at 700°C, RHA-Ru700 showed some degree of crystallization. The Scanning Electron Microscopy (SEM) micrographs showed the formation of well-defined flat elongated nano-sized rods with a smooth outer surface among the amorphous powder. RHA-Ru had a specific surface area of ca. 65 m^2 g^{-1}, while RHA-Ru700 had only ca. 10 m^2 g^{-1}, which is consistent with the formation of rod shaped crystalline phase. Both samples had pores in the mesoporous range. The Fourier transform infrared (FTIR) spectrum showed the presence of NO_3^- groups in RHA-Ru which was not present in RHA-Ru700. The Brunner Emmet Teller (BET) isotherm showed both samples had H3 hysteresis. Energy Dispersive Spectrometry (EDX) analysis showed that the distribution of Ru in the silica matrix was not homogeneous in RHA-Ru, however, it was found to be more homogeneous in RHA-Ru700.*

Keywords: rice husk ash, heterogeneous catalyst, ruthenium catalyst, sol-gel

1.   INTRODUCTION

Rice husk is a by-product of the rice milling industry. It is a unique crop residue with uniform size and high content of ash (14–25%). The silica content of the rice husk ash (RHA) can be as high as 90–97% [1–3]. Amorphous silica is well known and commonly used as a support material due to its high surface area, which will provide sufficient surface area for any metal to disperse [4]. There are very limited publications on the use of RHA as a matrix for preparing metal supported heterogeneous catalyst [5–10]. In all reported cases, the incipient-wet method and ion exchange methods were used to physically incorporate the metal into the rice husk silica matrix.

In recent years, considerable attention has been given to methods in which organic and inorganic catalytic surfaces are chemically modified in order to increase their usefulness in catalytic processes. The materials resulting from such chemical modifications have considerable potential as alternatives to conventional homogeneous and heterogeneous catalysts. Immobilization of transition metal complexes and metal clusters both provide reliable routes to a type of heterogeneous catalyst whose nature and mechanism may be more readily understood and potentially offer ways to manipulate metal particle and crystallite size to achieve new types of catalytic reactions [11].

More recently, ruthenium catalysts have attracted significant interest. These involve soluble complexes as well as solid catalysts. The most efficient Ru-based heterogeneous system for the aerobic oxidation of alcohols in a liquid phase includes recently developed Ru-Co-Al hydrotalite, Ru-hydroyapatite and Ru/Al$_2$O$_3$. Ruthenium catalysts are known to be sufficiently selective to avoid over oxidation of aldehydes to acids and are tolerant towards many functional groups that may be present in the alcohol molecules [12]. Oxides of ruthenium, used to prepare the heterogeneous catalysts can be very expensive. The cost of the catalyst can be reduced if the metal or its oxide can be dispersed in an inert matrix with a large surface area. This will reduce the amount of metal used and hence reduce the cost of the catalyst while the metal can be dispersed over a large surface area for effective and more efficient catalytic activity.

This paper reports the use of RHA as an inert material with a large surface area where the metal or its oxide is chemically incorporated and dispersed throughout the matrix. In previous studies, the RHA had been chemically modified with aluminium(III) ions via the precipitation technique. The resulting RHA-Al was shown to be a good adsorbent for palmytic acid [13]. Similarly, RHA-Fe and RHA-Fe700 was prepared and shown to be an active catalyst in the Friedel-Crafts benzylation of toluene with benzyl chloride [14]. This work details the preparation and characterization of Ru ions chemically incorporated into the rice husk silica matrix using the precipitation method. The prepared RHA-Ru catalyst was found to have a unique structure, which was very different from RHA-Al and RHA-Fe reported previously.

2.   EXPERIMENT

2.1   Raw Material

Rice husk obtained from a local rice milling company was first washed thoroughly with water to remove the adhering soil and dust. It was then dried under sunlight for 48 hours. The dried husk was then oxidized in a muffle furnace at 500ºC for 5 hours to produce white silica ash. The silica ash was stirred in 1.0

M HNO$_3$ for 24 hours and washed thoroughly with distilled water. The silica was designated as RHA.

## 2.2   Sample Preparation for RHA-Ru and RHA-Ru700

A 5 g sample of RHA was stirred in 250 ml of 6.0 M NaOH for 12 hours at room temperature and the solution was filtered to obtain sodium silicate solution. The solution was filtered to remove undissolved particles. It was then titrated with 3.0 M HNO$_3$ containing 10 wt% of metal [ruthenium(III) chloride] very slowly with constant stirring until pH 5.0 was reached. A soft gel was formed and the gel was aged for one day. After the aging process, the gel was filtered through suction filtration and washed with excess distilled water. It was then dried in an oven at 110ºC for 24 hours. The dried solid was manually ground in a mortar and labeled as RHA-Ru. In a typical synthesis, the mass of solid obtained was ca. 11.68 g. Sufficient amount of RHA-Ru was calcined at 700ºC for 5 hours and denoted as RHA-Ru700.

2.3   Sample Characterization

The prepared samples were characterized by Fourier transform infrared (FTIR) spectroscopy, Brunner Emmet Teller (BET) surface area analysis, powder X-ray Diffractometry, Scanning Electron Microscopy (SEM) and Energy Dispersive Spectrometry (EDX).

3.   RESULTS AND DISCCUSION

RHA obtained from the burning of the husk yielded white silica powder. The silica powder obtained is almost similar to that of the commercial silica gel in terms of the functional groups, the amorphous nature and also the physical structure [1,2,13–17]. Generally, RHA silica contains metal oxides [1]. Treatment with concentrated HNO$_3$ helps to reduce the impurities and leach out the metal oxides by forming nitrates which are easily dissolved in water. The acid treated rice husk ash, denoted as RHA, dissolves in sodium hydroxide producing sodium silicate solution, as shown in Eq. (1), where x is a variable that gives the ratio of the SiO$_2$ to Na$_2$O in the sodium silicate solution that affects its properties [18].

$$x\text{SiO}_2 \ + \ 2\text{NaOH} \ \rightarrow \ \text{Na}_2\text{O}{:}x\text{SiO}_2 \ + \ \text{H}_2\text{O} \qquad (1)$$
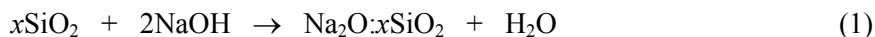
The sodium silicate solution was neutralized using nitric acid containing the metal to produce silica gel with the metal ion chemically incorporated into the silica matrix.

The surface structure of RHA-Ru and RHA-Ru700 were examined by the SEM. The SEM micrographs of the samples are presented in Figure 1. Figure 1(a) shows the amorphous structure of RHA-Ru at 2.00 K magnification, indicating a general porous matrix. The BET specific surface area for RHA-Ru was determined to be 65.10 m^2 g^{-1} (see Table 1). Upon calcination, the surface structure of RHA-Ru700 showed marked changes although maintaining a network of porous structure. The BET surface area of RHA-Ru700 was reduced to 10.38 m^2 g^{-1}. However, the bulk structure of RHA-Ru700 retained the amorphous matrix but this was interspersed with the presence of fine needles which were observed to be rather elongated. The SEM micrograph of RHA-Ru700 shows the existence of these fine needles. On further magnification [Fig. 1(c)], the needles looked like thin flat elongated pieces of fiber with sharp edges and of nano dimension.
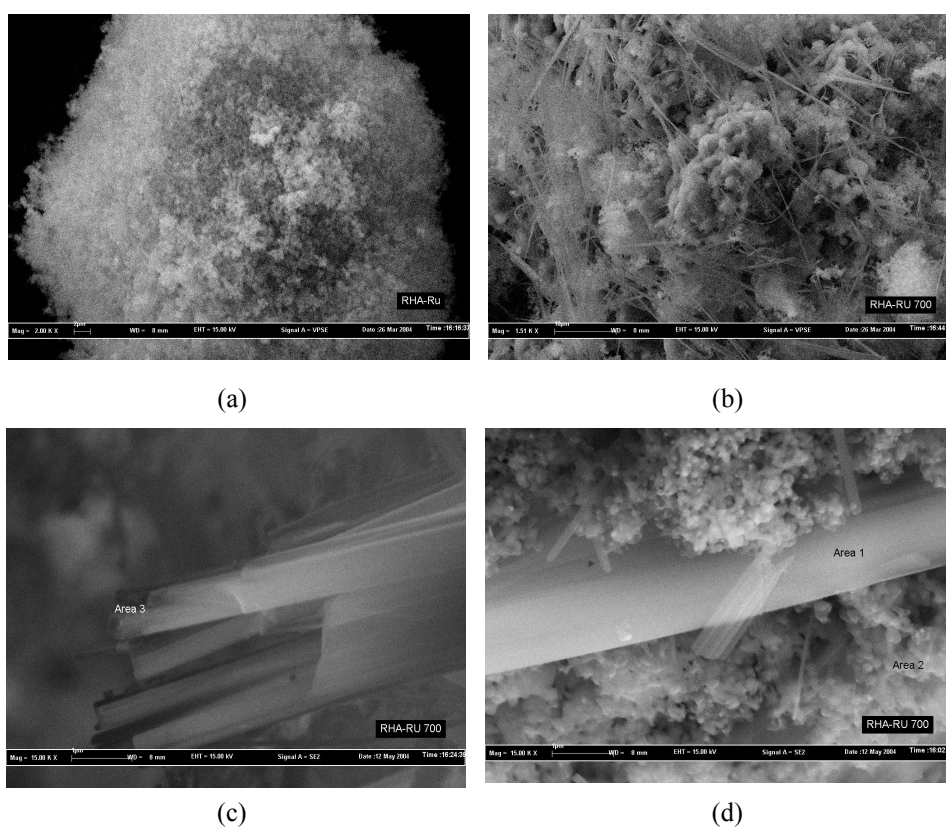

(a)   (b)

(c)   (d)

Figure 1: SEM images of RHA-Ru and RHA-Ru700, (a) RHA-Ru (× 2.00 K); (b) RHA-Ru700 (× 1.5 K); (c) RHA-Ru700 at 15 K magnification showing the ends of the flat fibers, and (d) RHA-Ru700 at 15 K magnification showing the flat fibers along its length

The width of the needles can be estimated to be about 200 nanometers with the length stretching several micrometers. The fibers which are crystalline are also seen to be very flexible as observed in Figure 1(b). Figure 1(c) shows the RHA-Ru700 fibers at 15,000 times magnification showing the well defined sharp edges of a typical crystalline solid. The flat and long nature of the fibers is evident from Figure 1(d) of the micrograph.

Figure 2 shows the XRD of RHA-Ru. There are no sharp peaks. A strong broad peak is observed at about 22º 2θ angle. This generally indicates that the solid is either not crystalline or it consists of microcrystalline structures. Amorphous substances display an atomic arrangement that is either random or has a very short-range order. This is indeed seen in the SEM micrographs in Figure 1.
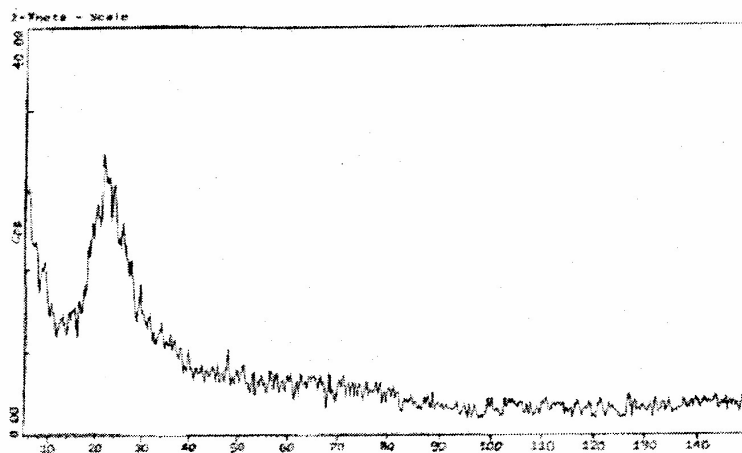

Figure 2: The X-ray powder diffraction of RHA-Ru

Figure 3 shows the XRD of RHA-Ru700. The existence of several sharp peaks indicates the presence of crystalline phase in the matrix. Crystallization had taken place due to the high temperature employed during the calcination. The SEM micrographs clearly indicate that this crystalline phase is due to the fine fibers observed in Figure 1. This unique fiber-like structure of RHA-Ru700 was not found in any of the other metal-supported RHA samples similarly prepared earlier [13,14,19] in our studies. The crystallization of RHA-Ru700 had resulted in the decrease of the surface area as shown in Table 1.
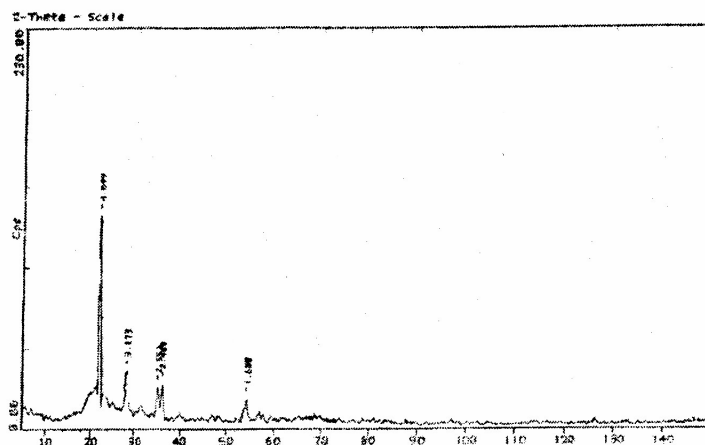
Figure 3: X-ray powder diffraction of RHA-Ru700

The distribution of the metal was found to be non homogenous for both RHA-Ru. More homogeneous distribution of the metal was observed in RHA-Ru700. EDX analysis (not included) on different spots on the fibers showed different composition of Ru. The composition of metal in RHA-Ru varied from 1.67 to 10.2%. Upon calcination, RHA-Ru700 had a narrower range of metal composition, which is between 2.50 to 5.80%. The greater homogeneity of Ru in RHA-Ru700 can be attributed to the fact that calcination removes the NO_3^- (by oxidation to gaseous oxides of nitrogen) ions and adsorbed water molecules from its pores (as indicated in the FTIR spectra in Fig. 4). This results in a much more homogeneous distribution of the elements in the solid. In both samples, the metal was thought to be strongly bonded in the porous RHA matrix. This conclusion was drawn due to the fact that the Ru remained in the matrix even after copious washing with distilled water. The Ru was thus not present as the original nitrate salt, which would have been washed away if it was present.

The major chemical groups present in RHA-Ru and RHA-Ru700 were identified by the respective FTIR spectrum. As can be seen in Figure 4, in general, the Infrared (IR) spectra of both samples had a broad band in the region of 3450–3500 cm^{-1} due to the surface O-H vibration. This band is due to the silanol, SiO-H groups and the HO-H vibration of the adsorbed water molecules bound to the silica surface. These modified silica gels are basically a high moisture product made up of a network of interconnected pores with a silicon dioxide core consisting of the silanol groups [18]. This surface silanol groups are responsible for physically adsorbing water molecules and holding them in place by hydrogen bonding. The water entrapped in the core, the silanol hydroxyl

groups and the physically adsorbed water together represent the moisture content in the silica gel samples.

The bending vibration for H-O-H was observed at 1637 cm^{-1} and this value corresponds to that reported in the literature [19]. This band still appears even though the samples were dried at 110ºC before the spectra were recorded. This is due to the moisture trapped in the narrow pores of the silica matrix. The strong band at 1099 cm^{-1} is due to the structural siloxane framework, which is the vibration frequency of the Si-O-Si bond. This peak shifted to 1109 cm^{-1} after calcinations, which is normally observed in these types of samples. This band was observed in both RHA and metal incorporated RHA and is the most prominent characteristic of any silica material having the Si-O-Si bond as the back bone. The band at 802 cm^{-1} was assigned to symmetric Si-O-Si stretching vibration [20] and this shifted to 795 cm^{-1} upon calcination. The Si-OH groups generally have a weak shoulder at around 980 cm^{-1}. By adding metal to silica, it results in a weak shoulder at 950 cm^{-1}. Maxim recently prepared Fe-doped silica and attributed this shift to the presence of Fe-O-Si bond [21]. In this work too, a peak at 960 cm^{-1} was observed in the RHA-Ru sample. However, it disappeared on calcination at 700ºC and thus it was not observed in RHA-Ru700. The disappearance of the band at 960 cm^{-1} occurs gradually as the calcination temperature is increased, as can be observed from the FTIR spectrum of RHA-Ru500 (RHA-Ru calcined at 500ºC for 5 hours) and RHA-Ru700. Given these observations, the band at 960 cm^{-1} in RHA-Ru cannot be confirmed as that of the stretching vibration of Ru-O-Si bond [21] as concluded by Maxim for the Fe-O-Si bond. The work done by Stark et al. [20] on titanium doped silica also proved to be inconclusive on the assignment of this particular band in the IR spectrum.

From Figure 4, it can be seen that there is a slight shoulder at about 543 cm^{-1} in the FTIR spectrum of RHA-Ru. This shoulder becomes less prominent as the calcination temperature is increased to 500ºC and completely disappears at 700ºC. Calcination at 700ºC results in a new band at 619 cm^{-1} as seen in the FTIR spectrum of RHA-Ru700. It is suggested that this band could be due to the stretching vibration of Ru-O-Si bond that is likely to be present in RHA-Ru700, although further confirmatory work need to be done. Nevertheless, a band at this wave number was never observed in RHA.

The FTIR spectrum of RHA-Ru exhibits a sharp peak at 1384 cm^{-1}, which is due to the vibrations of NO_3^- anion. This assignment is in agreement with literature [18,22] to our previous reported work [13]. This band too can be seen to progressively decrease as the calcination temperature is raised until it completely disappears at 700ºC.
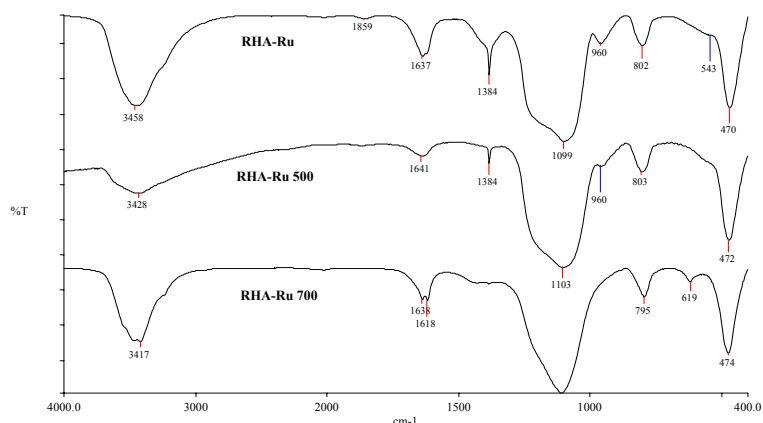
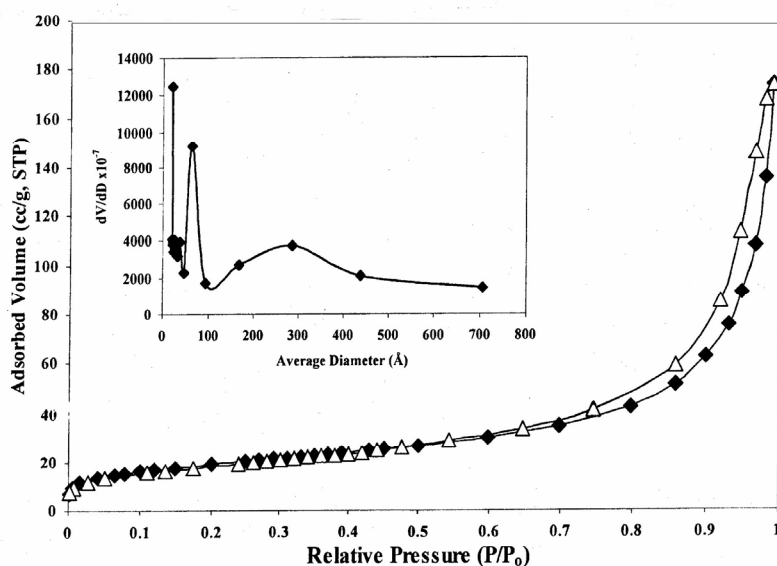Figure 4: The FTIR spectra of RHA-Ru and RHA-Ru700

Figure 5: The nitrogen adsorption isotherm for RHA-Ru

Notes: ♦ is the adsorption branch, and Δ is the desorption branch. Inset: the pore distribution graph of RHA-Ru

     The N_2 adsorption and desorption isotherms of both RHA-Ru and RHA-Ru700 are shown in Figures 5 and 6, respectively. In the nitrogen adsorption isotherm for both samples, the desorption branch does not follow the adsorption branch, but gives a distinct hysteresis loop, where the amount adsorbed is greater along the desorption branch compared to the adsorption

branch. The hysteresis loop can be classified as type H3 according to the International Union of Pure and Applied Chemistry (IUPAC) classification [23]. Generally, this type of hysteresis loop is believed to be found in solids with agglomerates, having slit-shaped pores. This model is assumed to have slab geometry with slit walls comprised of two infinite graphitic planes [24]. Similar results were obtained with RHA-Al and RHA-Al(C) [13].

From the pore distribution graphs shown (inset of Fig. 5), there are two distinct pore size distributions for RHA-Ru. These are between 40 and 100 Å and between 150 to 400 Å. Both these ranges fall within the mesoporous region.
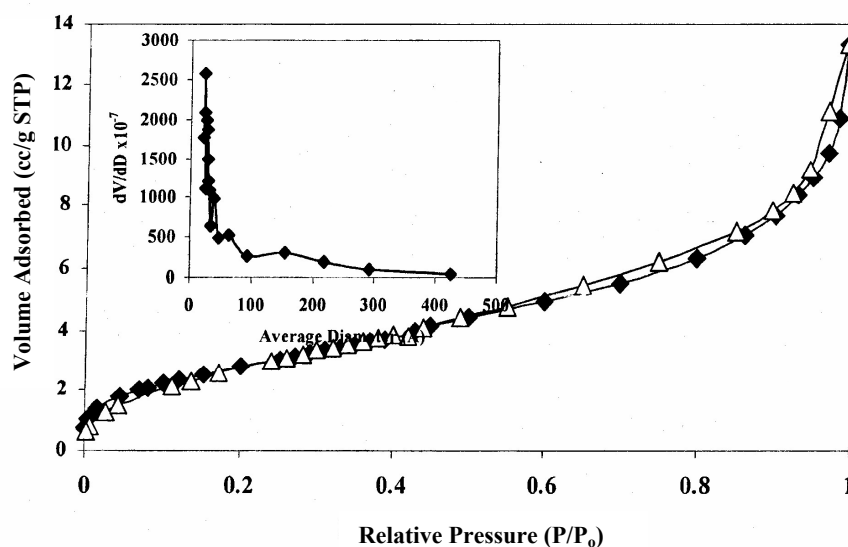

Figure 6: The nitrogen adsorption isotherm for RHA-Ru700

Notes: ♦ is the adsorption branch, and Δ is the desorption branch. Inset: the pore distribution graph of RHA-Ru700

After calcination, the pore distribution of RHA-Ru700 was found to be very different from RHA-Ru. From the inset of Figure 6, there are five different pore ranges. The first narrow range was from 20 to 25 Å. The second narrow pore range was from 25 to 35 Å. The third narrow pore range was from 35 to 50 Å. There are two wider pore ranges from 50 to 80 Å and the last was from 100 to about 200 Å. These pore sizes were not observed in RHA-Ru. This could be because of the adsorbed and trapped water molecules together with the NO_3^- ions clogging up the pores in RHA-Ru. However, on calcination, these molecules were either released by evaporation or decomposed to gaseous forms in the case of the nitrate ions, thus exposing these narrow pores in RHA-Ru700.

The BET surface area of RHA-Ru and RHA-Ru700 are given in Table 1. Both samples have reasonably high specific surface area. In general, the support material with a higher surface area implies a higher dispersion [11]. However, the average pore size and the pore volume of a sample will also affect the dispersion and reactivity of the sample [18].

Table 1: BET surface area of RHA-Ru and RHA-Ru700

	RHA-Ru	RHA-Ru700
BET surface area ($m^2\ g^{-1}$)	65.10	10.38
BJH Cumulative desorption pore volume ($m^3\ g^{-1}$)	0.251	0.0148
BJH desorption average pore diameter (Å)	146	67.28
BJH cumulative desorption surface area of pores between 17.00 and 300.0 Å ($m^2\ g^{-1}$)	68.7	8.80

Upon calcining at 700ºC, the RHA-Ru700 showed a decrease in the BET surface area. The decrease in surface area is influenced by the pore size of the sample. This is because, above 700ºC, inter-particle condensation of free hydroxyl groups occurs, which combines with the rearrangement of silica globules to produce a more stable configuration. Obviously, this inter-particle condensation is highly favored by smaller pores, resulting in faster collapse of pore structure [23]. The cumulative pore volume also shows a marked decrease (94.1%) in RHA-Ru700 in line with the fact that the micro pores would have collapsed first as the calcination temperature of the material increases to 700ºC. Likewise, the average pore size (diameter) in RHA-Ru700 was found to be much smaller, which is 67.28 Å, compared to 146 Å in RHA-Ru. With the decrease in the micropores as the calcination temperature is increased, the cumulative desorption pore area between the pore sizes of 17.0 to 300 Å also showed a decrease at the higher temperature, which is consistent with the collapse of the micropores.

4.   CONCLUSION

A simple and low energy method has been developed to produce a newer type of Ru-based heterogeneous catalyst supported on rice husk ash-silica. These potential catalysts were successfully prepared through the simple precipitation technique. The interaction between metal and silica support was believed to be via strong chemical metal-oxygen bonding. The Ru-based samples prepared have reasonably high surface area. Calcination resulted in the formation of nano sized

fibers which was apparently rather flexible. These materials should show good potential as heterogeneous catalysts. Further studies to increase the surface area and on the catalytic activity of these samples are in progress in our laboratory.

5. ACKNOWLEDGEMENTS

6. REFERENCES

1.   Farook, A. (1991). Preparation and adsorption studies on rice husk ash. M.Sc. thesis, Universiti Sains Malaysia, Pulau Pinang.
2.   Saleh, M.I., Farook, A. & Ab. Rahman, I. (1990). Production and characterization of rice husk ash as a source of pure silica. In R. Othman (Ed.). *Seramik Nusantara.* Pulau Pinang: Universiti Sains Malaysia, 261–273.
3.   Della, V.P., Kühn, I. & Hotza, D. (2002). Rice husk ash as an alternative source for active silica production. *Materials Letters*, 57, 818.
4.   Mekhemer, G.A.H., Abd-Allah, H.M.M. & Mansour, S.A.A. (1999). Surface characterization of silica-supported cobalt oxide catalyst. *Colloids and Surfaces*, A160, 251.
5.   Chang, F.W., Hsiao, T.J., Chung, S.W. & Lo, J.J. (1997). Nickel supported on RHA – Activity and selectivity in CO_2 methanation. *Applied Catalysis A: General*, 146, 225.
6.   Chang, F.W. & Tsay, M.T. (2000). Characterization of rice husk ash-supported nickel catalyst prepared by ion exchange. *Applied Catalysis A: General*, 203, 15.
7.   Chang, F.W., Tsay, M.T., Kuo, M.S. & Yang, C.M. (2002). Characterization of nickel catalyst on RHA-Al_2O_3 composite oxides prepared by ion exchange. *Applied Catalysis A: General*, 226, 213.
8.   Chang, F.W., Tsay, M.T. & Kuo, M.S. (2002). Effect of thermal treatments on catalyst reducibility and activity in nickel supported on RHA-Al_2O_3 systems. *Thermochim. Acta*, 386, 161.
9.   Chang, F.W., Kuo, W.Y. & Lee, K.C. (2003). Dehydrogenation of ethanol over copper catalyst on rice husk ash prepared by incipient wetness impregnation. *Applied Catalysis A: General*, 246, 253.

10.   Chang, F.W., Kuo, M.S., Tsay, M.T. & Hsieh, M.C. (2003). Hydrogenation of CO_2 over Ni catalyst on rice husk ash-alumina prepared by incipient wetness impregnation. *Applied Catalysis A: General*, 247, 309.

11.   Joel, M.S. (1982). *Chemically modified surfaces in catalysis and electrocatalysis*. ACS Symposium Series 192. Washington. D.C.: American Chemical Society, 1.

12.   Musawir, M., Davey, P.N., Kelly, G. & Kozhevniko, I.V. (2003). Highly efficient liquid-phase oxidation of primary alcohols to aldehydes with oxygen catalyzed by Ru-Co oxides. *Chem. Commun.*, 1414.

13.   Farook, A. & Chua, J.H. (2004). The adsorption of palmytic acid on rice husk ash chemically modified with Al(III) ion using the sol-gel technique. *J. Colloid and Interface Sci.*, 280, 55–61.

14.   Farook, A., Kalaivani, K. & Saraswathy, B. (2004). A novel iron loaded heterogeneous catalyst from rice husk ash silica for the Friedel-Craft benzylation of toluene with benzyl chloride using the sol-gel technique. Paper presented at the Regional Conference of Young Chemist (RCYC 2004), April 13–14, 2004, Universiti Sains Malaysia, Pulau Pinang, Malaysia.

15.   Farook, A. & Saleh, M.I. (1994). Adsorption isotherms of fatty acids on rice hull ash in a model system. *J. Am. Oil Chemists. Soc.*, 71, 1363.

16.   Farook, A. & Ravendran, S. (2000). Saturated fatty acid adsorption by acidified rice hull ash. *J. Am. Oil Chemists Soc.*, 77, 437.

17.   Farook, A. & Saleh, M.I. (1993). The removal of FFA from CPO and adsorption of palmytic acid on rice husk ash. In M.R. Nordin, K.Y. Liew, & A.A. Zainal (Eds.). *Surface science and heterogeneous catalysis*. Pulau Pinang: Penerbit Universiti Sains Malaysia, 99.

18.   Kamath, S.R. & Proctor, A. (1998). Silica gel from rice hull ash: Preparation and characterization. *Cereal Chem.*, 75, 484–487.

19.   Unger, K.K. (1979). Porous silica – Its properties and use as support in column liquid chromatography. *Journal of Chromatography Library*, 16(11). Amsterdam: Elsevier Scientific Publishing Company.

20.   Stark, W.J., Strobel, R., Gunther, D., Pratsinis, S.E. & Baiker, A. (2002). Titania-silica doped with transition metals via flame synthesis: Structural properties and catalytic behavior in epoxidation. *J. Mater. Chem.*, 12, 3620.

21.   Maxim, N. (2002). Metal silsesquioxanes as precursors to microporous metallosilicates. Ph.D. thesis. Einhoven University of Technology, The Netherlands.

22.   Ebsworth, E.A.V., Rankin, D.W.H. & Cradock, S. (1991). *Structural methods in inorganic chemistry* (2nd ed.). Oxford, UK: Blackwell Scientific Publication, 222.

23.   Leofanti, G., Padovan, M., Tozzola, G. & Venturelli, B. (1998). Surface area and pore texture of catalysts. *Catalysis Today*, 41, 207–219.

24.   Vansant, E.F., Voort, P.V.D. & Vrancken, K.C. (1995). *Characterization and chemical modification of the silica surface*. Amsterdam, Netherlands: Elsevier Science B.V., 93(22).